J Appl Electrochem (2009) 39:2481–2488
DOI 10.1007/s10800-009-9945-8

ORIGINAL PAPER

Time-averaged concentration calculations in pulse electrochemical machining, spectral approach

Nico Smets · S. Van Damme · D. De Wilde · G. Weyns · J. Deconinck

Received: 6 October 2008 / Accepted: 5 June 2009 / Published online: 24 June 2009

Abstract Simulation of the species concentrations during the pulse electrochemical machining (PECM) process can provide information on system design and guidelines for practical use. In detailed numerical calculations, the concentrations will be calculated simultaneously with the temperature due to mutual dependencies. The pulses that are applied to the PECM system have to be described on a timescale that can be orders of magnitude smaller than the physical timescales in the system. If the full detail of the applied pulses has to be taken into account, the time accurate calculation of the variable distributions' evolutions in PECM can become a computationally very expensive procedure. A different approach is used by time averaging the pulses applied to the system. Performing this, the timesteps used during the calculations are no longer dictated by the pulse characteristics. Using this approach is computationally very cheap, yet satisfying results can be obtained. In the previous study of the authors (Smets et al., J Appl Electrochem 37(11):1345–1355, 2007 [8]), the hybrid calculation and the quasi-steady-state shortcut (QSSSC) were introduced. These methods introduce errors, however, which were quantified using analytical solutions and found to be acceptable. The results applied only to rectangular pulses. In this study, the more general case of arbitrary pulse forms is considered using a spectral approach. The concentration and the temperature calculation have different requirements for optimal approximated calculations, and a compromise has to be found between them. An analysis is performed on a simplified model, which provides useful guidelines during simulations.

Keywords Pulse electrochemical machining · Concentration distribution evolution · Time averaging · Transient · Spectral approach

List of symbols

A	Pulse scale factor (mol m^{-3})
c	Concentration (mol m^{-3})
$\overline{c}$	Averaged concentration (mol m^{-3})
$\tilde{c}$	Concentration ripple (mol m^{-3})
c_{decay}	Concentration decaying component (mol m^{-3})
D	Diffusion coefficient (m^2 s^{-1})
E	Error function (%)
F	Faraday constant (=96,485 C mol^{-1})
J	Current density distribution (A m^{-2})
n	Spectral component index (−)
t	Time (s)
T	Pulse period (s)
T'	Dimensionless pulse period (−)
$\overline{v}$	Velocity vector (m s^{-1})
x	Distance (m)
z	Valence (−)
α	Duty cycle (−)
δ	Nernst diffusion layer thickness (m)
τ	Time constant (s)
Φ_c	Mass flux (mol s^{-1} m^{-2})
ψ	Pulse delay (s)
ψ^*	Optimal pulse delay (s)
ψ_{lim}	Limit pulse delay (s)
ω	Angular frequency (s^{-1})

N. Smets (✉) · S. Van Damme · D. De Wilde · G. Weyns · J. Deconinck
IR/ETEC Department, Vrije Universiteit Brussel, Pleinlaan 2, 1050 Brussels, Belgium
e-mail: nsmets@vub.ac.be

1 Introduction

Electrochemical machining (ECM) is a manufacturing process based on the controlled anodic dissolution of a metal at large current densities (in the range of 1 A mm^{-2}). An electrolyte is used to carry away the produced heat and mass, among other reaction products.

Despite its advantages, some difficulties still trouble the application of ECM. One important issue is the lack of quantitative simulation software to predict the tool shape and machining parameters necessary to produce a given work-piece profile [4–6]. The most complete model needs to deal with the effects of the fluid flow, gas evolution, heat generation, the electrochemical processes at the electrodes, the transport of the species involved, and all this while the electrode shape changes. This study makes a contribution in calculating the species' concentrations.

Pulse electrochemical machining (PECM) involves the application of current or voltage pulses. One wishes to apply pulses for reasons of accuracy and surface quality [1–3, 6].

In order to simulate electrochemical processes with pulses, one has to perform calculations with boundary conditions that vary in time. By applying a time-stepping algorithm, all the variable distributions are calculated in time. The applied pulses have to be described on a time-scale that can be orders of magnitude smaller than the timescale on which physical effects in the system evolve. This means that a lot of timesteps would have to be calculated to perform a satisfying simulation, which would be a computationally very expensive procedure.

A solution to this problem is given in [8], where the temperature evolution was calculated. The hybrid calculation was introduced in the work as an economical solution to the problem. It consists of applying the averaged boundary conditions first, and applying pulses starting from a time of interest t^*. A special case of the hybrid calculation is the quasi-steady-state shortcut (QSSSC), where the averaged SS is used as a starting state, and pulses are applied afterward. It was shown that delaying the start of the pulses in time with a certain value ψ influences the accuracy of the approximative method. Analytical formulae for optimal values of ψ were presented in the study. Also, a function E was defined to quantify how well the QSS is approximated, by using the QSSSC.

The hybrid method was applied for the calculations of concentration in [9]. The study in [9] applied only to rectangular pulses. In this study, the hybrid method is studied while applying arbitrary pulse shapes. A general formulation is made, which applies for any possible pulse shape. Two specific pulse shapes are considered for further investigations: a full-wave rectified sine and a half-wave rectified sine, see Fig. 1a and b. When current pulses are applied, the concentration production pulses will have the same shape. When voltage pulses are applied, the shape of the concentration production pulses will change a bit due to non-linear relations; hence, a slightly different spectrum will be obtained. This distortion is, however, too complex to be considered under general circumstances, and is neglected.

When performing a simulation and calculating the temperature and concentrations simultaneously, a different optimal pulse delay ψ^* will be needed for optimal approximative calculations for each variable. Only one ψ^* can be applied, however, and a compromise has to be found to achieve optimal results. This problem will be addressed in this article.

Secondary reactions of the produced species are not considered.

2 Mathematical model

The concentration distribution evolution $c(\overline{r}, t)$ in the system is calculated using a convection–diffusion equation,

$$\frac{\partial c}{\partial t} + \overline{v} \cdot \overline{\nabla} c = \overline{\nabla} \cdot \left(D \overline{\nabla} c \right). \tag{1}$$

Mass production is considered at the electrode, and is imposed as flux Φ_c at the electrode surfaces contiguous to the electrolyte.

$$\Phi_c = D \frac{\partial c}{\partial x} = \frac{J}{zF}. \tag{2}$$

The efficiency is 100%, i.e., all the current is considered to be consumed for the production of c.

3 Averaging the analytical solution of a simple problem

The problem will be described in one spatial dimension (1D). One electrode is considered. The electrode is regarded as surrounded by an adherent layer of electrolyte of uniform thickness through which diffusion takes place [7], i.e., a Nernst diffusion layer. The Nernst diffusion layer is a linear approximation for the true diffusion layer. The closer it is to the electrode, the better is the approximation, see Fig. 2.

In the Nernst diffusion layer, only diffusion is considered, reducing Eq. 1 to

$$\frac{\partial c}{\partial t} = D \frac{\partial^2 c}{\partial x^2}. \tag{3}$$

Concentration $c(x,t)$ will be produced at the contact surface between the electrode and the electrolyte, giving rise to the boundary condition

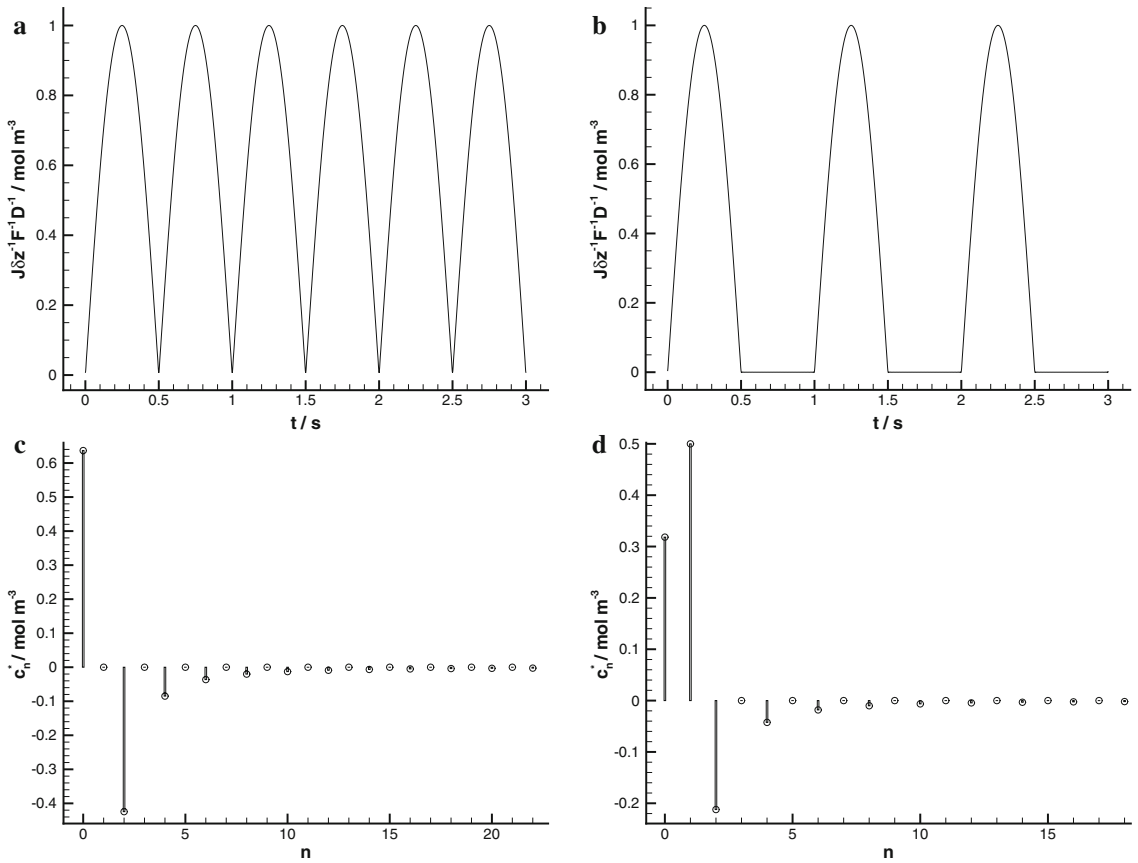

Fig. 1 Pulse shapes and their spectra ($A = 1$ mol m^{-3}). **a** Full-wave rectified sine. **b** Half-wave rectified sine. **c** Full-wave rectified sine spectrum. **d** Half-wave rectified sine spectrum

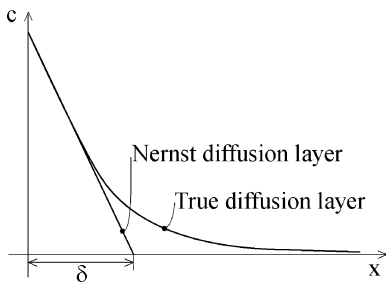

Fig. 2 Nernst diffusion layer and true diffusion layer. Steady-state case

$$\left.\frac{\partial c}{\partial x}\right|_{x=0} = \frac{J(t)}{zFD}. \tag{4}$$

The initial condition is that $c = 0$ at $t = 0$. We also have $c = 0$ at $x = \delta$, where δ is the thickness of the Nernst diffusion layer.

An arbitrary pulse shape can be written by means of a Fourier series. Hence, the boundary condition at the electrode will be written as

$$\frac{J(t)\delta}{zFD} = \sum_{n=0}^{\infty} c_n^* \cos(n\omega t + \phi_n), \tag{5}$$

where c^*_n and ϕ_n can be calculated when the pulse shape is defined, and where

$$\omega = \frac{2\pi}{T}. \tag{6}$$

The spectrum for a full-wave rectified sine is

$$\begin{cases} c_0^* = \frac{2A}{\pi} & \\ c_1^* = 0 & \\ c_n^* = \frac{2A}{\pi}\frac{(-1)^n+1}{1-n^2} & n = 2,3,4,\ldots \\ \phi_n = 0 & n = 0,1,2,\ldots \end{cases} \tag{7}$$

The spectrum for a half-wave rectified sine is

$$\begin{cases} c_0^* = \frac{A}{\pi} & \\ c_1^* = \frac{A}{2} & \\ c_n^* = A\frac{(-1)^n+1}{\pi(1-n^2)} & n = 2,3,4,\ldots \\ \phi_n = 0 & n = 0,2,3,\ldots \\ \phi_1 = -\frac{\pi}{2} & \end{cases} \tag{8}$$

The spectrum of a rectangular pulse is

$$\begin{cases} c_0^* = A\alpha \\ c_n^* = \frac{2A}{\pi n}\left|\sin(\alpha\pi n)\right| & n = 1,2,3,\ldots \\ \phi_0 = 0 \\ \phi_n = \mathrm{atan2}(-1, \tan^{-1}(\alpha\pi n)) & n = 1,2,3,\ldots \end{cases} \quad (9)$$

The atan2(y,x) function computes the principal value of the arc tangent of y/x, using the signs of both arguments to determine the quadrant of the return value.

The concentration evolution in the diffusion layer is then (based on the result from [7])

$$c(x,t) = \overline{c}(x,t) + \tilde{c}(x,t) + c_{\mathrm{decay}}(x,t), \quad (10)$$

where the averaged component $\overline{c}(x,t)$ is

$$\overline{c}(x,t) = c_0^* \sum_{k=1}^{\infty} \beta_k(x)(1 - \mathrm{e}^{-t/\tau_k}), \quad (11)$$

the ripple $\tilde{c}(x,t)$ (with zero average) is

$$\tilde{c}(x,t) = \sum_{n=1}^{\infty} c_n^* \sum_{k=1}^{\infty} \beta_k(x) \frac{\cos(n\omega t + \phi_n - \mathrm{atan2}(n\omega\tau_k, 1))}{\sqrt{1 + n^2\omega^2\tau_k^2}}, \quad (12)$$

and the decaying contribution $c_{\mathrm{decay}}(x,t)$ is

$$c_{\mathrm{decay}}(x,t) = -\sum_{n=1}^{\infty} c_n^* \sum_{k=1}^{\infty} \beta_k(x) \times \frac{\cos(\phi_n - \mathrm{atan2}(n\omega\tau_k, 1))}{\sqrt{1 + n^2\omega^2\tau_k^2}} \mathrm{e}^{-t/\tau_k}, \quad (13)$$

with

$$\beta_k(x) = \frac{8}{\pi^2(2k-1)^2} \cos\left(\frac{(2k-1)\pi}{2}\frac{x}{\delta}\right), \quad (14)$$

$$\tau_k = \frac{4\delta^2}{\pi^2 D(2k-1)^2}. \quad (15)$$

Note that

$$\sum_{k=1}^{\infty} \beta_k(x) = 1 - \frac{x}{\delta}. \quad (16)$$

It is possible to combine averaged boundary conditions and pulsed boundary conditions in one calculation. These calculations are called hybrid [8]. Starting from $t = 0$, the averaged concentration fluxes are applied, and after time $t = t^*$, pulses are applied (possibly delayed by ψ). It can be shown that the concentration evolution is composed of the averaged component $\overline{c}(x,t)$, a ripple $\tilde{c}(x,t-t^*)$ and a decaying component $c_{\mathrm{decay}}(x, t-t^*)$, where the latter two start from the time $t = t^*$:

$$c_{\mathrm{hybrid}}(x,t) = \overline{c}(x,t) + \tilde{c}(x,t-t^*) + c_{\mathrm{decay}}(x,t-t^*). \quad (17)$$

A particularly interesting case is when $t^* \to \infty$. The starting state at $t = t^*$ is then the averaged SS. This situation is called the QSSSC. When performing the QSSSC, it is convenient to start the pulsed calculation from $t = 0$, while applying the averaged SS in the initial state. Note that in this case, the averaged concentration reduces to $\overline{c}(x,t) = c_0^*(1 - \frac{x}{\delta})$:

$$c_{\mathrm{QSSSC}}(x,t) = c_0^*\left(1 - \frac{x}{\delta}\right) + \tilde{c}(x,t) + c_{\mathrm{decay}}(x,t). \quad (18)$$

When the concentration production initially starts, the decaying component is naturally present, cfr. Eq. 10. Using the approximative hybrid method, a significant reduction in numerical time stepping can be obtained. When we apply the hybrid calculation and start pulsing at $t = t^*$, the presence of the decaying component (cfr. Eqs. 17 and 18) is not natural at all. The decaying component c_{decay} should have started already at $t = 0$, instead of at $t = t^*$, and chances are that it would have largely decayed or even totally disappeared at $t = t^*$. The presence of the decaying component $c_{\mathrm{decay}}(x,t)$ troubles the approximative hybrid method and introduces errors. Assume that at the time of interest $t = t^*$, the decaying component c_{decay} in the full calculation would be already very small or even zero. The hybrid method would then yield good approximative results, if it would be possible to eliminate $c_{\mathrm{decay}}(x,t)$ during the hybrid calculation.

The decaying component $c_{\mathrm{decay}}(x, t)$ can be manipulated by delaying the pulses in time with an amount ψ. It can easily be shown that when the pulse is delayed by ψ then

$$\frac{J(t-\psi)\delta}{zFD} = \sum_{n=1}^{\infty} c_n^* \cos(n\omega t + \phi_n - n\omega\psi); \quad (19)$$

hence, to delay the pulse by ψ, one needs to replace the phase ϕ_n by $\phi_n - n\omega\psi$ in expressions 5, 12, and 13.

The optimal value for ψ, written as ψ^*, can then be calculated by minimizing $|c_{\mathrm{decay}}(x,t)|$ in Eq. 13, and calculating for which ψ this occurs. This is an optimization problem. In order to simplify, only the component $k = 1$ is considered. This component is the largest in amplitude, and the slowest to damp out. When the spectral content of the pulse shape is relatively low, another simplification can be done: the optimization problem can be limited to the most important spectral component. This approach is very pragmatic, but it does have the advantage that it delivers a practical closed form expression for ψ^*. This pragmatic approach proves to be very sufficient in this study. For the case of the full-wave rectified sine, the major spectral component is at double frequency ($n = 2$), and the optimal pulse delay is then

$$\psi^* = \frac{1}{2\omega}\left(\frac{3\pi}{2} - \mathrm{atan2}(2\omega\tau_1, 1)\right). \quad (20)$$

For the case of the half-wave rectified sine, the major spectral component is at pulse base frequency ($n = 1$), and the optimal pulse delay is

$$\psi^* = \frac{1}{\omega}(\pi - \text{atan2}(\omega\tau_1, 1)). \tag{21}$$

For slow systems, where the first and largest time constant τ_1 is very large compared to the period T, the optimal pulse delay simplifies to

$$\psi_{\lim} = \lim_{\frac{T}{\tau_1}\to 0} \psi^* = \frac{T}{4}, \tag{22}$$

for both the full-wave rectified and the half-wave rectified sine.

For rectangular pulses, the spectral content can be fairly large, especially when the duty cycle α becomes small. When determining ψ^* it is not justified to limit the calculation to only one spectral component, one has to consider all the spectral components that are substantially contributing. In the previous study [9], an optimal pulse delay for rectangular pulses was obtained:

$$\psi^* = \tau_1 \ln\left(\alpha \frac{1 - e^{T/\tau_1}}{1 - e^{\alpha T/\tau_1}}\right). \tag{23}$$

Performing the optimization on Eq. 13 delivers the same result, but expression 23 has the advantage to be in a closed form, and is superior for practical use.

The transient concentration evolution, together with the QSSSC, is calculated for a half-wave-rectified sine-pulsed case where $x/\delta = 0.4$ and $T' = 0.20$, where

$$T' = \frac{TD}{\delta^2}. \tag{24}$$

By not delaying the pulses in time, the results from Fig. 3 are obtained. By delaying the pulses with ψ^*, the results from Fig. 4 are obtained. It can be seen that by delaying the pulses with ψ^*, $c_{\text{decay}}(x,t)$ can be reduced significantly.

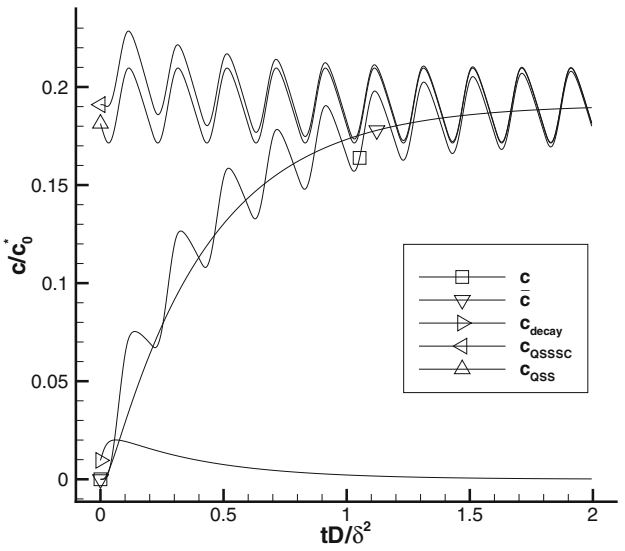

Fig. 3 Concentration evolution, $\psi = 0$ (half-wave rectified sine pulses, $T' = 0.20$, $x/\delta = 0.4$)

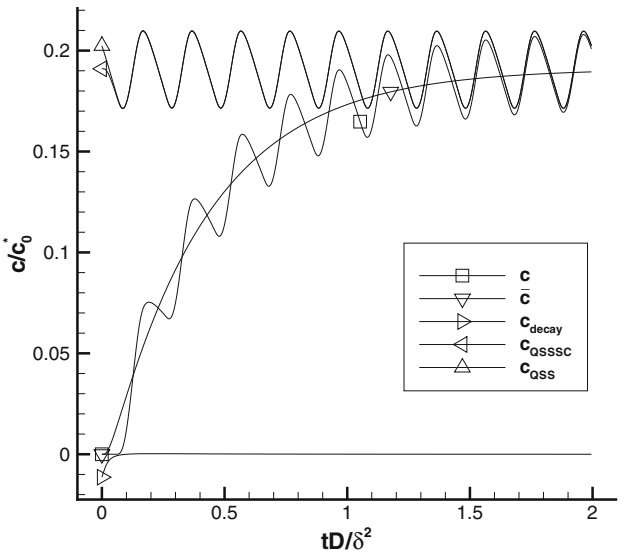

Fig. 4 Concentration evolution, $\psi = \psi^*$ (half-wave rectified sine pulses, $T' = 0.20$, $x/\delta = 0.4$)

Since the full transient calculation and the QSSSC contain exactly the same $c_{\text{decay}}(x, t)$, only the QSSSC will be studied from here. The more accurate the QSSSC approximates the real QSS, the better. The difference between the QSSSC and the QSS will be quantified with the error function E (in %) [8], which is defined as

$$\begin{aligned} E_j &= \frac{\int_{\delta_j} |c_{\text{QSSSC}}(x,t) - c_{\text{QSS}}(x,t)| \mathrm{d}t}{\int_{\delta_j} c_{\text{QSS}}(x,t) \mathrm{d}t} \times 100 \\ &= \frac{\int_{\delta_j} |c_{\text{decay}}(x,t)| \mathrm{d}t}{\int_{\delta_j} c_{\text{QSS}}(x,t) \mathrm{d}t} \times 100, \end{aligned} \tag{25}$$

where the integrals are calculated over δ_j, which is the jth on-time. The integration domain is limited to the on-times, because this is the only interval of interest while performing calculations for PECM. During the on-time of the pulse, the actual shape change of the workpiece occurs, which is the ultimate goal for simulations on PECM. The states during the off-times are of no primary importance.

For x/δ from about 0.6–1, the solution in Eq. 10 gives a permanent underestimation for the real $c(x, t)$. This can also be seen in Fig. 2 for the SS case. It has to be noted that the impact of this underestimation is limited on the accuracy of E. Apart from the underestimation, the shape of $c(x, t)$ is fairly accurate, and because the ratio is taken between two underestimated values, the underestimation is largely canceled out. For x/δ greater than 1, no other results than the approximation $c(x > \delta, t) = 0$ are available with this method, and hence no conclusions on E can be made.

E_j is mainly a function of T', x/δ, and the pulse shape. Two additional parameters are the number of on-time j, and ψ. E_1 is shown in Fig. 5 for $\psi = 0$, and in Fig. 6 for the same setup, but with $\psi = \psi^*$.

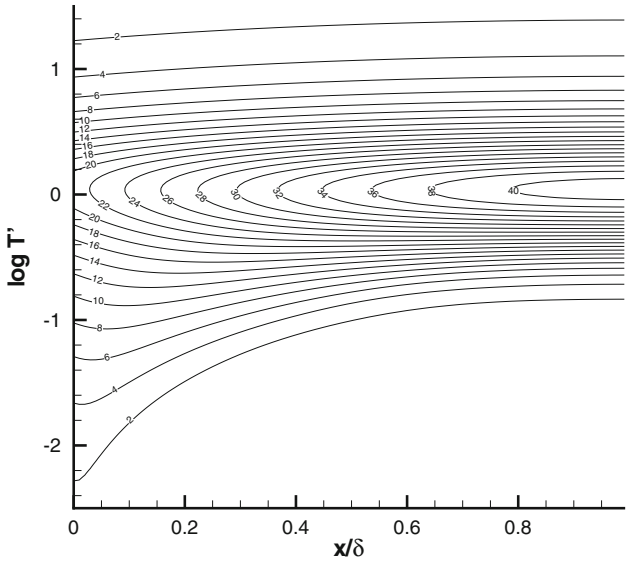

Fig. 5 E_1 as a function of T' and x/δ, half-wave rectified sine pulsing. $\psi = 0$

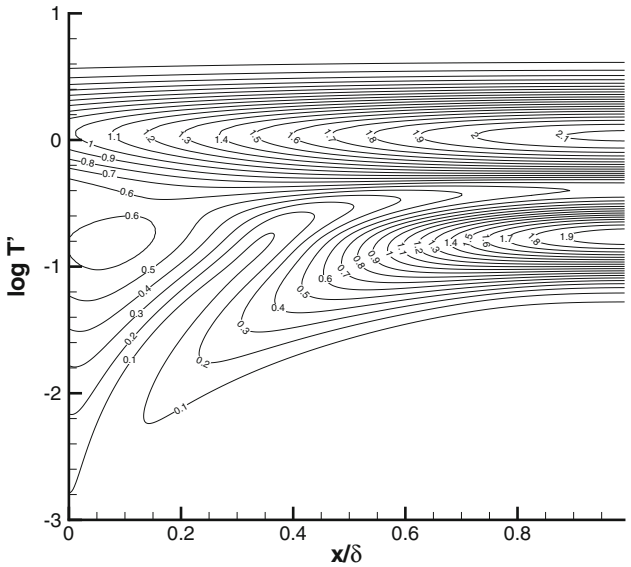

Fig. 6 E_1 as a function of T' and x/δ, half-wave rectified sine pulsing. $\psi = \psi^*$

Many figures like Figs. 5 and 6 can be produced. In order to be able to draw a general conclusion about the errors introduced by the approximative method, the worst-case values of E encountered will be summarized in a table. For a full-wave rectified sine, the worst-case values can be seen in Table 1. For a half-wave rectified sine, the worst-case values can be seen in Table 2.

With the full-wave rectified sine pulsing, it can be seen in Table 1 that the errors introduced by the decaying component are not very large. Delaying the pulses in time with a delay ψ^* does not dramatically reduce the error further. The pulse delaying does not have a great impact with the full-wave rectified sine pulsing. This is because of the fairly large DC component, and the first important spectral component being at double base frequency ($n = 2$), while there is a zero component at the base frequency.

Table 1 Full-wave rectified sine, worst-case values of E

ψ	E_1 max (%)	E_2 max (%)
0	3.49	0.147
ψ_{lim}	2.97	0.132
ψ^*	0.68	0.033

Table 2 Half-wave rectified sine, worst-case values of E

ψ	E_1 max (%)	E_2 max (%)
0	41.1	10.4
ψ_{lim}	8.16	1.23
ψ^*	2.13	0.35

With the half-wave rectified sine pulsing, it can be seen in Table 2 that the worst-case value of E, encountered with $\psi = 0$, is about 41%, which is not acceptable. Calculating until the second on-time during the QSSSC, we could still encounter a maximum E_2 of about 10%, which is still unacceptable. By delaying the pulses with $\psi = \psi^*$, the worst-case values of E are strongly reduced. It can be seen from Table 2 that the maximum error E_1 is about 2%, which is already acceptable, since in many cases, the uncertainties on the thermal parameters of the system are also of this order. Calculating until the second on-time gives a maximum possible E_2 of about 0.35%, which is quite satisfactory.

For rectangular pulses, the method in this study can be used to reproduce the results from the former study of the authors [9].

For the temperature evolution in the system also, an optimal ψ^* exists to minimize the decaying component on the temperature evolution [10]. The pulse delay for the concentration and the temperature has to be taken the same, since they result from the same current pulses. Since the time constants of the temperature evolution are generally much larger than those of the concentration evolution, the temperature gets priority in choosing the pulse delay ψ. The cases where the present averaging technique is very important are the cases where the slowest time constant τ_1 of the temperature evolution is much larger than the pulse period T. For this case, the expression for ψ^* simplifies to

$$\lim_{\frac{T}{\tau_1}\to 0} \psi^* \approx \frac{T}{4} = \psi_{\text{lim}}. \tag{26}$$

The evolution of ψ^* is shown in Fig. 7. In the temperature case, we are generally at the left of the curve. The concentration case will generally be more to the right on the T/τ_1 axis. It can be seen on Fig. 7 that when ψ^* for the concentration deviates most from ψ_{lim}, the point is more to the right on the T/τ_1 axis, i.e., $T \gg \tau_1$, which makes that the concentration does not accumulate over multiple pulses, and hence, pulse shifting has become of no importance. Due of this, the error E stays limited for the concentration calculations when $\psi = \psi_{\text{lim}}$ is applied, as can be seen in Fig. 8 for E_1. The case where $\psi = \psi_{\text{lim}}$ is also noted in Tables 1 and 2. It can be seen that, however, the pulse delay is not optimally chosen, the decaying component is still acceptably low, if the calculation is continued until the second on-time.

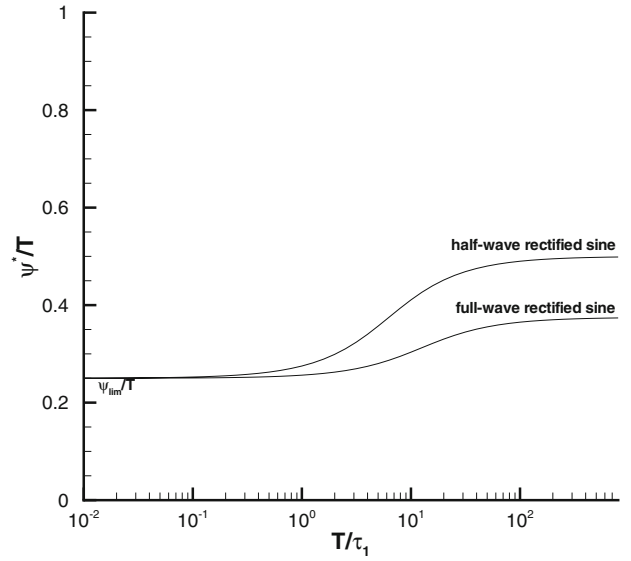

Fig. 7 $\frac{\psi^*}{T}$ as a function of $\frac{T}{\tau_1}$, full-wave and half-wave rectified sine pulsing

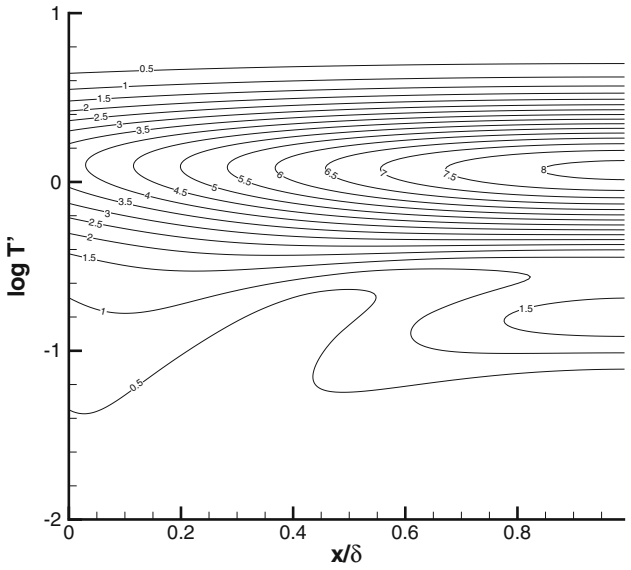

Fig. 8 E_1 as a function of T' and x/δ, half-wave rectified sine pulsing. $\psi = \psi_{\text{lim}}$

4 Conclusions

The applied averaging technique adopted in the earlier study for the calculation of temperature transients in electrochemical systems during PECM is adopted in this study for the calculation of concentration transients.

For concentration calculation, this averaging technique is generally not of vital importance, because the transient is usually not very long. The idea is to combine both the temperature and concentration calculations in one step, and hence the averaging technique gets applied to the concentration evolution as well.

The averaging technique applies very well to the concentration evolution, but the problem arises that the calculation of the temperature and concentrations require different optimal pulse shifts ψ^*. As generally the slowest time constant τ_1 of the temperature evolution is longer than the slowest time constant τ_1 of the concentration evolution, priority is given to the temperature calculation. This proves to be a good compromise for the theoretical case treated in this article. When the slowest time constant τ_1 of the temperature evolution is much larger than the pulse period T, the compromise made in the choice of $\psi = \psi_{\text{lim}}$ performs well for the pulse shapes considered in this study. Already during the second on-time in the QSSSC, the calculated variables are acceptable. The general formulation is capable of analyzing any pulse shape.

The assumptions of the models, used to derive the analytical solutions, are too strict for real-life ECM conditions. Nevertheless, very interesting conclusions are made, which will be used in the future study. The results also apply very well as practical rules of thumb, when using the hybrid technique during complex numerical calculations.

References

1. Datta M, Landolt D (1981) Electrochemical machining under pulsed current conditions. Electrochim Acta 26(7):899–907
2. Kozak J (2004) Thermal models of pulse electrochemical machining. Bull Pol Acad Sci 52(4):313–320
3. Kozak J, Rajurkar K (1991) Computer simulation of pulse electrochemical machining (PECM). J Mater Process Technol 28 (1–2):149–157
4. Lohrengel M, Klueppel I, Rosenkranz C, Betterman H, Schultze J (2003) Microscopic investigations of electrochemical machining of Fe in NaNO3. Electrochim Acta 48(20–22):3203–3211

5. Mount A, Clifton D, Howarth P, Sherlock A (2003) An integrated strategy for materials characterisation and process simulation in electrochemical machining. J Mater Process Technol 138:449–454
6. Rajurkar KP, Zhu D, McGeough JA, Kozak J, De Silva A (1999) New developments in electro-chemical machining. Ann CIRP 48(2):567–579
7. Rosebrugh TR, Lash Miller W (1910) Mathematical theory of the changes of concentration at the electrode brought about by diffusion and by chemical reaction. J Phys Chem 14(9):816–884
8. Smets N, Van Damme S, De Wilde D, Weyns G, Deconinck J (2007) Time averaged temperature calculations in pulse electrochemical machining, part I: theoretical basis. J Appl Electrochem 37(11):1345–1355
9. Smets N, Van Damme S, De Wilde D, Weyns G, Deconinck J (2008) Time averaged concentration calculations in pulse electrochemical machining. J Appl Electrochem 38(11):1577–1582
10. Smets N, Van Damme S, De Wilde D, Weyns G, Deconinck J (2009) Time averaged temperature calculations in pulse electrochemical machining, spectral approach. J Appl Electrochem 39(6): 791–798